Nonlinear optical characterization of tetraphenylporphyrin in the picosecond regime

C. Cassagne, M. Chniti, Cid de Araújo, H. Belmabrouk, Georges Boudebs

Nonlinear Optical Characterization of Tetraphenylporphyrin in the Picosecond Regime

C. Cassagne [(1)], M. Chniti [(1,2)], Cid B. de Araújo [(3)], H. Belmabrouk [(2)], and G. Boudebs [(1,*)]

[(1)] *LUNAM Université, Université d'Angers, LPhiA, EA 4464, 2 Boulevard Lavoisier, 49045 Angers France*
[(2)] *Laboratory Electronic and Microelectronic, University of Monastir, Tunisia*
[(3)] *Departamento de Física, Universidade Federal de Pernambuco, 50670-901 Recife, PE, Brazil*
[(*)] *Tel:(33) 2.41.73.54.26, Fax:(33) 2.41.73.52.16, email: georges.boudebs@univ-angers.fr*

ABSTRACT

Applying the D4σ-Z-scan technique with a laser delivering single pulses in the picosecond regime at 1064 nm, 532 nm, and 355 nm we report on the nonlinear (NL) optical properties of 5,10,15,20-Tetraphenyl-21H,23H-porphine (TPP) and 5,10,15,20-Tetraphenyl-21H,23H-porphine zinc (ZnTPP) solutions prepared in chlorobenzene. Accurate measurements of the NL coefficients for 4 concentrations in both compounds are provided. The results show no response in the IR for both materials, negative NL refraction for TPP in the green changing sign to positive for ZnTPP and positive NL refraction in the UV for both compositions. The NL absorption of these materials is quite huge in the visible range where applications for optical limiting are needed.
Keywords: porphyrin**,** nonlinear absorption, nonlinear refractive index, D4σ-Z-scan technique.

1. INTRODUCTION

Large Porphyrins (Pphs) are biological macromolecules that play a crucial role in various processes in nature such photosynthesis and oxygen transport in cells, as well as applications such as in solar photovoltaic devices [1] and photodynamic cancer therapy [2]. Synthesis and experimental investigation of nonlinear (NL) optical properties of Pphs have been reported by several groups [3, 4]. The large interest in the NL properties of Pphs is due to their unique electronic, optical and biochemical properties [5, 6] as well as the high stability and architectural flexibility that provide a very good basis to finely tune their optical response.

In the present article, we report on experiments with TPP and ZnTPP using an Nd: YAG laser operating in the picosecond regime at 10 Hz repetition rate to measure the nonlinear absorption (NLA) coefficients and NL refractive indices of the Pphs based solutions at three different wavelengths (1064 nm, 532 nm and 355 nm) and four different concentrations. The experiments were performed calculating the beam waist relative variation (BWRV) using D4σ intensity profile measurements combined to Z-scan method [7]. It is referred here as D4σ-Zscan technique [8]. It was possible to determine the sign and the magnitude of the NL refractive indices even in the presence of high NLA at relatively high concentration which is the case when dealing with Pphs. Simple linear relations were empirically obtained allowing a correlation between the NL parameters and the linear absorption coefficient.

2. EXPERIMENTAL

2.1 UV-VIS Absorption
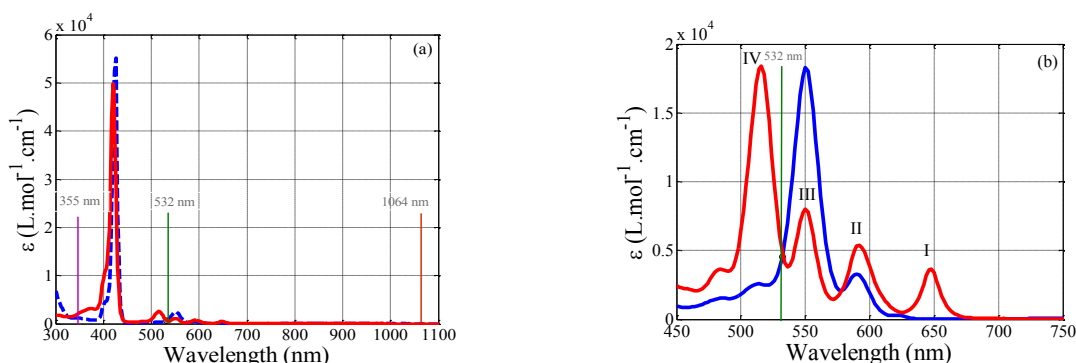
Figure 1: Molar extinction coefficients ε versus wavelengths. Solid (red) line for TPP; dashed (blue) line for ZnTPP. Porphyrin concentrations for both compounds: (a) 10^{-4} mol/L; (b) 10^{-3} mol/L. The vertical straight lines indicate the laser wavelengths at 1064 nm, 532 nm and 355 nm. I, II, III, IV are the TPP Q-bands.

The electronic absorption spectra were recorded in chlorobenzene solution. Figure 1(a) shows the optical absorption spectrum of TPP in solid (red) line and ZnTPP dashed (blue) line measured from 300 nm to 1100 nm, at room temperature. The strong absorption band centered at $\approx$ 420 nm ($\approx$ 2.96 eV) is called Soret band (also

called B band). Figure 1(b) shows the spectra of the samples measured at concentration of 10^{-3}M. The bands in the region from ≈ 500 to ≈ 700 nm region are the Q bands that are attributed to transitions associated to the π-π* conjugate system. Also drawn in Fig. 1(a) are vertical lines that indicate the laser wavelengths used in the experiments. In Table 1 we indicated the wavelength corresponding to the maximum of absorption, λ_{max}, and the corresponding molar extinction coefficient for each band.

2.2 Nonlinear Measurements

The experimental setup used to implement the D4σ-Z-scan technique is described in details in [8]. For the characterization of the nonlinear refraction and absorption, the solution were inside a 1 mm thick quartz cell. The NL measurements were made at 355 nm, 532 nm and 1064 nm. The results are shown in Tables 1 and 2. At 1064 nm the TPP and ZnTPP solutions did not show any NL response even for high concentrations. Experiments were made at 15 GW/cm^2 in solutions with concentration of 10^{-3} M and for pure chlorobenzene. The measured NL refraction was approximately equal for the Pph solutions and for pure chlorobenzene. It was found $n_2 = (0.16 \pm 0.05) \times 10^{-18} \mathrm{m}^2/\mathrm{W}$ and $\beta < 0.02$ cm/GW which is smaller than the sensitivity of the apparatus. At 532 nm and $I_0 = 8.5$ GW/cm^2, chlorobenzene shows a NL refractive index equal to $n_2 = (0.35 \pm 0.05) \times 10^{-18} \mathrm{m}^2/\mathrm{W}$ and $\beta < 0.02$ cm/GW. The NL refraction behavior of TPP and ZnTPP is illustrated in Figs. 2(a) and 2(b), respectively; the data presented were obtained at 2.1 GW/cm^2. The BWRV profile with the peak after the valley indicates that the TPP presents a negative NL refractive index exhibiting self-defocusing at this wavelength. The open-aperture Z-scan data, presented as insets of both figures, illustrate the NLA behavior. These results illustrate clearly the influence of Zn on the NL response at 532 nm: (i) the sign of n_2 is positive for ZnTPP while it is negative for TPP; (ii) the 2PA coefficient of ZnTPP is larger than in TPP. Note that in Table 1 the positive value of n_2 for TPP is due to the low concentration (0.12×10^{-3} M) showing the result of the competition between the positive NL refraction due to chlorobenzene alone and the small amount of TPP molecules dissolved inside.
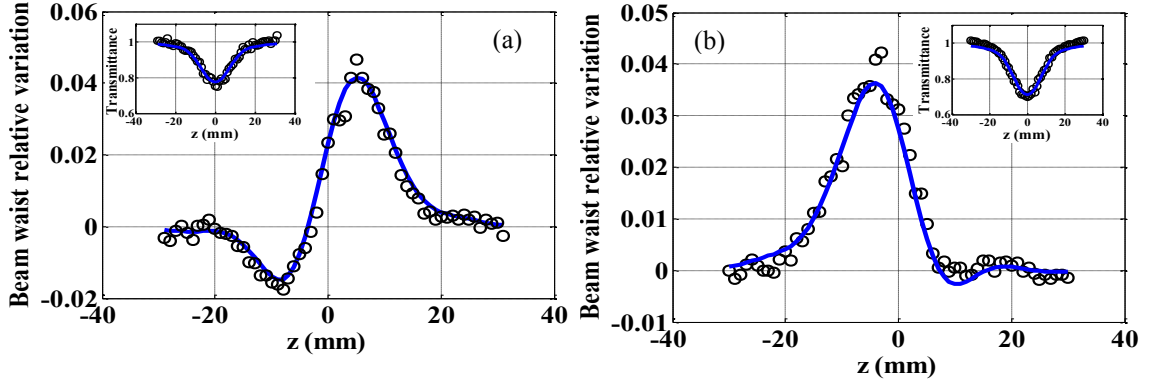

Figure 2: Beam waist relative variation versus z, the sample position at 532 nm. Sample thickness: 1 mm. Pph solution concentration:10^{-3} M. Laser intensity: I_0=2.1 GW/cm^2. (a) Sample: TPP (α=1126 m^{-1}); (b) sample: ZnTPP (α=1048 m^{-1}). The insets represent the open aperture Z-scan traces and the blue lines represent the best fit of the data.

At 355 nm the experiments with pure chlorobenzene gives $n_2 = (0.55 \pm 0.1) \times 10^{-18} \mathrm{m}^2/\mathrm{W}$ and $\beta = (0.35 \pm 0.06)$ cm/GW. Due to the high linear absorption coefficient ($\alpha = 4221$ m^{-1}) of Pph solution at concentration 10^{-3} M, the NL measurement at low intensity was not possible because even in the linear regime, in order to detect a signal at the CCD, the needed laser intensity was high enough to induce unwanted NLA leading to non-reliable coefficient values. The measurement was possible starting from concentration of 0.5×10^{-3} with $I_0 = 4$ GW/cm^2. TPP and ZnTPP solutions presented positive n_2 (self-focusing) and strong NLA. The measured NL parameters for solutions with different concentrations of TPP and ZnTPP are shown in Table1 for $\lambda = 532$ nm and in Table 2 for $\lambda = 355$ nm. The 2PA cross section, σ_2, was calculated from β, the NL absorption coefficient, using the relation $\sigma_2 \left(\mathrm{cm}^4 \cdot \mathrm{s} \cdot \mathrm{photon}^{-1} \right) = 10^3 \mathrm{h} \nu \beta / N \ C$, where N_A is the Avogadro number, C is the Pph concentration, h the Planck's constant and ν is the frequency of the incident light. The σ_2 values are indicated in Tables 1-2 in GM units (1 GM = 10^{-50} cm^4·s·photon^{-1}). Note that the values of σ_2 are not dependent on the Pph concentration, as expected.

Table 1. Linear and nonlinear parameters of TPP and ZnTPP (with different concentrations), at 532 nm. α_{532} is the linear absorption coefficient, n_2 is the effective NL refractive index, β is the NLA coefficient, I_0 is the laser peak intensity and σ_2 is the 2PA cross-section in GM units.

	Concentration ($\times 10^{-3}$M)	α_{532} (cm^{-1})	I_0 (GW/cm^2)	$n_2 \times 10^{-18}$ (m^2/W)	β (cm/GW)	σ_2 (GM)
Chlorobenzene			2.0 – 8.0	0.35 ± 0.05	< 0.06	
TPP	1	11.2		-2.7 ± 0.5	5.5 ± 0.8	3.4 ×10^5
	0.48	5.45	2.1	-0.9 ± 0.3	2.8 ± 0.4	3.6 ×10^5
	0.24	2.7		-0.26 ± 0.4	1.3 ± 0.3	3.4 ×10^5
	0.12	1.4		0.19 ± 0.1	0.7 ± 0.2	3.6 ×10^5
ZnTPP	0.94	10.4		1.7 ± 0.3	7.8 ± 0.1	5.1 ×10^5
	0.47	5.3	2.1	0.9 ± 0.2	4.0 ± 0.5	5.3 ×10^5
	0.23	2.7		0.6 ± 0.1	2.0 ± 0.3	5.4 ×10^5
	0.11	1.1		0.5 ± 0.1	1.0 ± 0.1	5.6 ×10^5

Table 2. Linear and nonlinear parameters of TPP and ZnTPP (with different concentrations), at 355 nm. α_{355} is the linear absorption coefficient, n_2 is the effective NL refractive index, β is the NLA coefficient, I_0 is the laser peak intensity and σ_2 is the 2PA cross-section in GM units.

	Concentration ($\times 10^{-3}$M)	α_{355} (cm^{-1})	I_0 (GW/cm^2)	$n_2 \times 10^{-18}$ (m^2/W)	β (cm/GW)	σ_2 (GM)
Chlorobenzene			7.6 - 25	0.5 ± 0.1	0.35 ± 0.06	
TPP	1	42.2		-	-	-
	0.48	20.4	4.0	2.8 ± 0.6	6.4 ± 0.8	1.2 ×10^6
	0.24	10.2		1.4 ± 0.2	3.5 ± 0.3	1.3 ×10^6
	0.12	5.2		0.8 ± 0.1	1.7 ± 0.2	1.3 ×10^6
ZnTPP	0.94	18.9		1.0 ± 0.2	7.3 ± 1	0.7 ×10^6
	0.47	9.4	4.0	0.6 ± 0.1	3.4 ± 0.5	0.7 ×10^6
	0.23	4.6		0.5 ± 0.1	1.8 ± 0.3	0.7 ×10^6
	0.11	2.2		0.4 ± 0.1	1.2 ± 0.2	1.0 ×10^6

   In Fig. 3, we summarized the values of the NL coefficients of TPP and ZnTPP at 532 nm and 355 nm as a function of the linear absorption coefficient, α (which is proportional to the Pph concentration). Figure 3(a) shows the variation of n_2 versus α for ZnTPP (data in blue color): empty squares at 355 nm, filled squares at 532 nm and for TPP (red data) empty circles at 355 nm, filled circles at 532 nm. At very low concentration (very low α), the intersection of the straight lines with the vertical axis occurs for a positive value of n_2 corresponding to pure chlorobenzene (within the experimental error). Figure 3(b) shows the variation of β versus α for ZnTPP (blue data): empty squares at 355 nm, filled squares at 532 nm and for TPP (red data) empty circles at 355 nm, filled circles at 532 nm. At very low concentration, the intersection of the straight lines with the vertical axis occurs at the value of β corresponding to pure chlorobenzene. Notice that the maximum efficiency for optical limiting is obtained at 532 nm. Indeed, for a given α the NLA is higher at 532 nm for both Pphs compositions when compared to the contribution obtained at 355 nm as noticed by the effective slope of the linear fits.
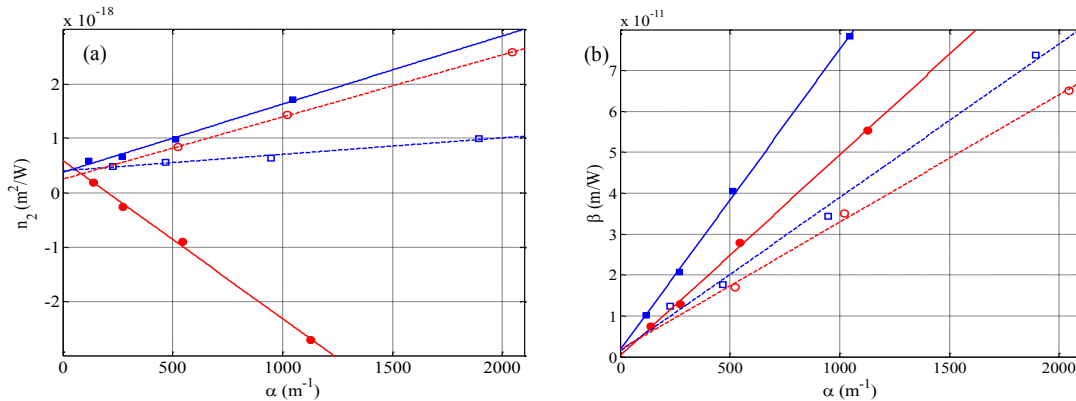

Figure 3: (a) Values of n_2 versus the linear absorption coefficient for ZnTPP: (blue data) empty squares in the UV (355 nm), filled squares in the green (532 nm) and for TPP (red data) empty circles in the UV (355 nm), filled circles in the green (532 nm). (b) Values of β versus the linear absorption coefficient for ZnTPP: (blue data) empty squares in the UV, filled squares in the green and for TPP (red data) empty circles in the UV, filled circles in the green. The dashed and solid lines are the linear fits.

2.3 Discussion

To investigate the contribution of the solvent, D4σ-Z-scan experiments were performed with pure chlorobenzene. As expected, no significant NL absorption was detected at 1064 nm and 532 nm; at 355 nm. The measured n_2 values show a normal dispersion behavior with respect to wavelengths. This decreasing behavior

with λ suggests the high reliability of the n_2 absolute values determined via the BWRV measurements [8] for transparent liquids far away from any absorption band. At 1064 nm both Pphs solutions did not show NLA because they are transparent at this wavelength. Although the energy of two laser photons falls into the Q bands region (see Fig. 1b) these bands are relatively weak. For excitation at 532 nm the energy of two photons corresponds to the energy of one photon at 266 nm that implies a large NLA.

Based on the results of [9] studying the same molecules and as in [10] we concluded that the effective third-order susceptibility governing the NL response of TPP and ZnTPP is due to a cascade process $\chi^{(1)} : \chi^{(1)}$ (acting as an effective third-order susceptibility). In this process the first $\chi^{(1)}$ is mainly related to the ground state absorption and the second $\chi^{(1)}$ is mainly influenced by the excited state refraction. The first excitation step is due to the bound electrons in the Pph molecules in the singlet S_0. The second step is dependent on the number of molecules in the excited singlet S_1 and is related to the change in the refractive index per unit photoexcited molecule. The population of the S_1 states will always be small due to their fast relaxation time [9].

Finally, the herein reported NLA coefficients when compared to other values found for organic compounds [11] are much larger. Furthermore the effective 2PA cross section values measured in the commercial Pphs are of the same order of magnitude than those reported for porphyrin supramolecules [12].

3. CONCLUSIONS

In summary, the third-order nonlinearity of TPP and ZnTPP was investigated applying the D4σ-Z-scan technique in the ps regime at 355 nm, 532 nm and 1064 nm. Beside a change of the NL refractive index from negative to positive due to the presence of Zn it was measured large NLA coefficients for both compounds. The NL behaviour observed indicates the large potential of TPP and ZnTPP for optical limiting applications because of their large 2PA cross-section of several thousand GM units. The NL response is attributed to an effective $\chi^{(3)}_{eff}$ dominated by a cascade process. The reported results indicate that ground state absorption and excited state refraction dominate in these experiments and therefore linear and effective 2PA strengths are linked.

REFERENCES

[1]   H. Imahori and S. Fukuzumi: Porphyrin and fullerene-based molecula*r* photovoltaic device, *Adv. Funct. Mater*. 2004, 14, 525.
[2]   B. Minaev and M. Lindgren: Vibration and fluorescence spectra of porphyrin-cored 2,2-bis(methylol)-propionic acid dendrimers, *Sensors*, 2009, 9, 1937.
[3]   M.O. Senge, M. Fazekas, E.G.A. Notaras, W.J. Blau, M. Zawadzka, O.B. Locos, and E.M.N. Mhuircheartaigh: Nonlinear optical properties of porphyrins, *Adv. Mater*. 2007, 19, 2737.
[4]   C.G. Liu, D.F. Zhang, M.L. Gao, and X.H. Sun: Computational study on second-order nonlinear optical properties of a series of axially substituted zinc porphyrin, *Comp. Theor. Chem*. 2013, 1027, 26.
[5]   Z. Valicsek and O. Horváth: Application of the electronic spectra of porphyrins for analytical purposes: The effects of metal ions and structural distortions, *Microchem. J*. 2013,107, 47.
[6]   N.M. Barbosa Neto, D.S. Correa, L. De Boni, G.G. Parra, L. Misoguti, C.R. Mendonça, I.E. Borissevitch, S.C. Zílio, and P.J. Gonçalves: Excited states absorption spectra of porphyrins-solvent effects, *Chem. Phys. Lett*. 2013, 587, 118.
[7]   M. Sheik-Bahae, A.A. Said, T.H. Wei, D. Hagan, and E.W. Van Stryland: Sensitive measurement of optical nonlinearities using a single Beam, *IEEE J. Quantum Electron*. 1990, 26, 4.
[8]   G. Boudebs, V. Besse, C. Cassagne, H. Leblond, C.B. De Araújo: Nonlinear characterization of materials using the D4σ method inside a Z-scan 4f-system, *Opt. Lett*. 2013, 38, 13.
[9]   W. Blau, H. Byrne, and W.M. Dennis: Reverse saturable absorption in tetraphenyl porphyrins, *Opt. Commun*. 1998, 56, 25-29.
[10] T.H. Wei, D.J. Hagan, M.J. Sence, E.W. Van Stryland, J.W. Perry, D.R. Coulter: Direct measurements of nonlinear absorption and refraction in solutions of phthalocyanines, *Appl. Phys. B*. 1992, 54, 46.
[11] L. De Boni, A.A. Andrade, S.B. Yamaki, L. Misoguti, S.C. Zilio, D.Z. Atvars Teresa, and C.R. Mendonca: Two-photon absorption spectrum in diazoaromatic compounds, *Chem. Phys. Lett*. 2008, 463, 360.
[12] K. Ogawa and Y. Kobuke: Nonlinear absorption by porphyrin supramolecules, in *Nonlinear Optics*, N. Kamanina (Ed.), ISBN: 978-953-51-0131-4, InTech, Available from: http://www.intechopen.com/books/nonlinear-optics/nonlinear-absorption-by-porphyrin-supramolecules.